Cavity QED in Ultra-Cold Strontium Atoms

B. Sc thesis by
Morten Herskind
dpm152@alumni.ku.dk

Supervised by Jan Westenkær Thomsen

Niels Bohr Institute

University of Copenhagen

June 2015

Abstract

This project reviews frequency stabilizing a laser used in an optical atomic clock. The first part of the thesis is dedicated to the theoretical background and generation of an error-signal used in a feedback-loop to frequency stabilize a laser. This error-signal is influnced by the experiment's surroundings, which introduces so-called RAM-noise.
The second part is devoted to the stabilization of the RAM-noise, as a mean to optimize the laser stabilization. The implementation of the noise-stabilization improves the long-term stability of the error-signal by one order of magnitude. The lower, not yet achievable, limit for the stabilization is found to be restricted by electronic equipment flicker noise. This limit is two orders of magnitude more stable on long time scales than the original RAM-noise limit.

Contents

1 Introduction **1**

2 Experimental Setup **1**
2.1 General overview 2
2.2 Electro-optic modulation 3
2.3 Narrowband laser light 4
2.4 Cavity-atom system and detection 7
2.5 Phase measurement profile 10

3 Residual amplitude modulation **11**
3.1 RAM control 13
3.2 RAM error signal and feedback control 14
3.3 Allan Variance 14

4 Data analysis and discussion **16**
4.1 PDH-lock stability 16
4.2 RAM stability 17

5 Conclusion **20**

6 References **21**

A Intensity signal from strontium filled cavity calculation **22**

B Allan deviation MatLab script **23**

1 Introduction

When Galileo examined falling bodies and pendulums, he tried to determine the time-dependencies of their motion. He did not have a clock at his disposal. Instead he measured time as fractions of his own heartbeat. This measurement is heavily loaded with uncertainty. The same basic approach to scientific work is taken in modern physics. However, the experiments are more advanced and require very precise time measurements on short timescales.
Today, clocks are used to measure time. A clock is basically a method of counting a regularly repeating process. Older clocks counted the swings of a pendulum. The period of a pendulum does not stay constant, therefore it is not a stable clock. In addition, the period is long, which means a pendulum clock cannot measure short time intervals.
To develop a very precise and stable clock, a physical process which is both fast and stable is needed. Light is a good example of such a process. Visible light has a frequency on the order of 10^{17} Hz.
This process only works if the light is monochromatic. The closest thing to a monochromatic light source is a laser. A laser, however, always has a linewidth, which means it has several frequency components. It is not possible to count the oscillations of just one component. The next best thing is to make sure it has as few components as possible. This is done by making a laser with a very narrow linewidth.
To make sure the laser frequency does not change over time, it is compared to a reference which does not change in time. An example of such a reference is an atomic transition.
This is the principle behind an optical atomic clock. To make sure the frequency is correct, the laser probes an atomic sample. If the atomic sample absorps, the frequency is correct, and the clock is reliable. If not, the laser frequency is adjusted until the atoms absorp again.
The development and improvement of optical atomic clocks have found applications in improved measurements of the geoid [1], and more exotic experiments as Gravitational-wave detection interferometers [2] and measurements of a possible drift in the fine-structure constant [3].

2 Experimental Setup

In order to frequency stabilize a light source, it is necessary to generate an error signal. A good error-signal has a steep slope and a sign-dependence corresponding to the direction of the error.
The main idea of stabilization is to send the error-signal back to an actuator via a feedback loop, to counter an unwanted drift. The idea behind feedback is described with a conceptual block diagram, see Figure 2.1. It is the process box that is stabilized.

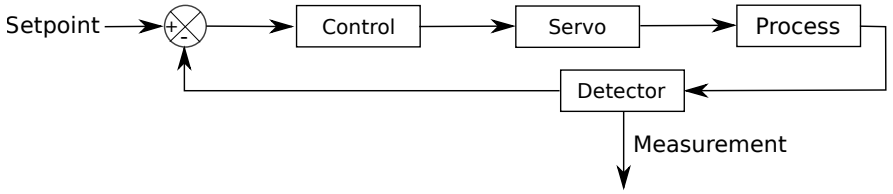

Figure 2.1: A block diagram consists of arrows which represent the signal, and conceptual boxes which are the elements of an experimental setup. The detector measures an analog signal, and gives out an electronic signal. The setpoint is the voltage that is being stabilized to. The circled box subtracts measurements and setpoint. If they are equal, no feedback signal is sent forward. The control box is an electronic circuit. This often consists of a frequency filter, amplification and a control circuit which manipulates the errorsignal. The servo is an actuator that performs the stabilization.

In this experiment, a laser is used to probe a cavity-atom system to generate the error-signal. The probe laser is stabilized with a PDH-lock [4] and the error-signal's noise is reduced with a feedback mechanism. The error signal's noise is what limits the stabilization.

2.1 General overview

There are three stages in the experiment. The first is the generation of narrow-band laser light, using feedback-control with an optical cavity and a tunable laser. This stage is the Pound-Drever-Hall(PDH) lock box in Figure 2.2. The box is a representation of the experimental setup in Figure 2.4. The second stage is a stabilization of the RAM noise in the electro-optic phase modulation(EOM) used in the main experiment. This modulation adds frequency sidebands to the narrow-band laser, called the carrier.
Stage 3 is a coupling between the laser beam and the strontium filled cavity-atom system. The cavity is filled by slowing down and trapping strontium atoms in a Magneto-Optical trap [5] . A slow gas is equivlent to a cold gas, which is why the experiment is called Cavity-QED (cQED) with ultra-cold strontium atoms. The coupling induces a phase in the carrier.This phase is used as the error-signal supplied to an AOM. An AOM is an Acousto-Optic Modulator which shifts the carrier frequency. The AOM stabilization is not yet experimentally realized.

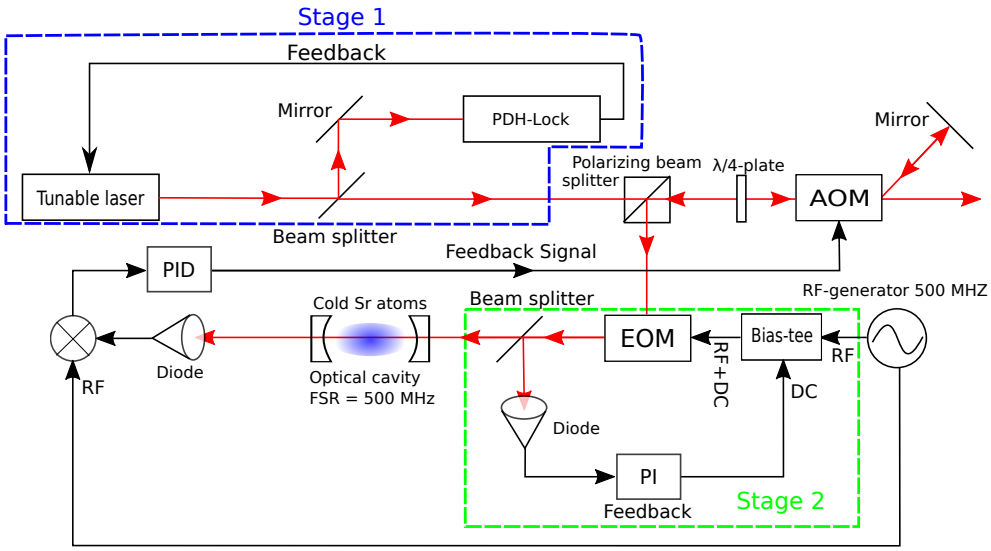

Figure 2.2: Full experiment: The experiment has three stages. A laser linewidth stabilization in the PDH-Lock. The second stage is electro-optic modulation in the EOM. There is a noise-reduction feedback loop in this stage as well. The last stage is the coupling of light and atoms in the cavity. The measured signal in diode 2 is used to frequency stabilize the light.

2.2 Electro-optic modulation

To generate the final error-signal used for stabilizing the frequency, the Noise-Immune Cavity-Enhanced Optical Heterodyne Molecular Spectroscopy (NICE-OHMS) [6] technique is used. The experimental setup realization is described in the previous section. This technique uses three frequency components; one carrier, and two evenly spaced sideband frequencies. The measured signal is the sum of the beat signals between the sidebands and the carrier, transmitted from the cQED-system. These two beat signals are exposed to the same noise in the experiment. When the beat signals are forced to be π out of phase, the noise cancels out when superposing the two signals. Ideally, it is noise-immune.

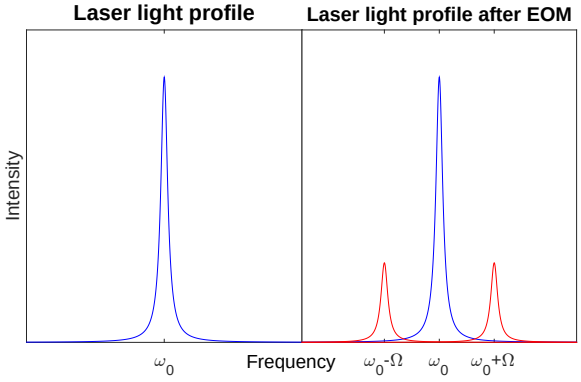

Figure 2.3: EOM profile: The sidebands are Ω displaced from the central frequency.

The effect of electro-optic modulation is seen in figure 2.3. The incoming light is phase modulated with an RF-frequency Ω. This is described by adding a phase which varies with the RF-frequency

Ω. An electric field entering the EOM

$$E = E_0 \cdot e^{i\omega_0 t}$$

becomes

$$E = E_0 \cdot e^{i\omega_0 t + i\beta \cdot \sin(\Omega t)} \tag{2.1}$$

By use of the Jacobi-Anger expansion this is

$$E = E_0 \cdot e^{-i\omega_0 t + i\beta \cdot \sin(\Omega t)} \tag{2.2}$$

$$= E_0 \cdot e^{i\omega_0 t} \cdot (J_0(\beta) + \sum_{k=1}^{\infty} J_k(\beta) e^{i\Omega t} + \sum_{k=1}^{\infty} (-1)^k J_k(\beta) e^{-i\Omega t}) \tag{2.3}$$

where $J_k(\beta)$ are Bessel functions of the first kind[7], which decrease rapidly in amplitude as k increases, so all $k > 1$ can be disregarded. β is called the modulation index. Varying this transfers energy between carrier and the sidebands, while never violating energy conservation. The $k = 1$ approximation leads to

$$E = E_0 \cdot J_0(\beta) e^{i\omega_0 t} + E_0 \cdot J_1(\beta) e^{i(\omega_0 + \Omega)t} - E_0 \cdot J_1(\beta) e^{i(\omega_0 - \Omega)t} \tag{2.4}$$

2.3 Narrowband laser light

The narrowband laser light is used to drive the ${}^1S_0 \rightarrow {}^3P_1$ transition of a strontium atom gas. From quantum mechanics [8] the possibility of this transition happening is proportional to:

$$|\langle {}^3P_1 | \mathbf{e} \cdot \mathbf{r} | {}^1S_0 \rangle|^2 = D_{S,P}$$

This is zero, which means that it is a dipole-forbidden transition. It is not impossible to excite an electron into the ${}^3P_1$ state, but it is rare. If the final and initial state are switched, which corresponds to emission from the ${}^3P_1$ state, the result is the same since $D_{S,P} = D_{P,S}$

If an electron has been excited, then it rarely de-excites. This means it has a long lifetime τ. A transition with a long lifetime has a narrow natural linewidth $\Delta\nu$ because of the relation

$$\Delta\nu \sim \frac{1}{\tau}$$

To drive a given transition, the driving field, in this case the laser beam, must have a linewidth close to the transition's. Stage 1 in the experiment is to generate light with a very narrow linewidth. This is done with a Pound-Drever-Hall lock as seen in Figure 2.4

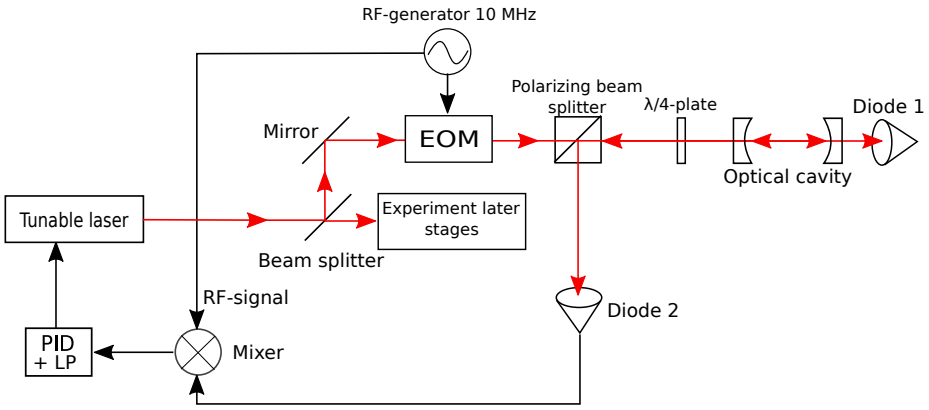

Figure 2.4: Pound-Drever-Hall Lock. This is a stabilization scheme as sketched in the block diagram in Figure 2.1. Relating the experiment to the block diagram the setpoint is zero, and the process is the laser linewidth of the red arrows. All the optical components and the EOM can be seen as part of the process, but they are passive and do not respond to the control signal. Diode 2 is the detector. The control box is the RF-generator, the mixer and the LP+PID box. The LP is a low-pass filter and the PID is a Proportional-Integrator-Differentiator circuit. The Servo box is the tunable laser.

The principle behind Pound-Drever-Hall locking is that light is only reflected back out of the cavity if it is out of resonance with the cavity. The resonance frequency of the cavity is an integer amount of the free spectral density, FSR, $\nu = m\frac{c}{2L}$. If the incoming frequency drifts off resonance, the reflected intensity increases.

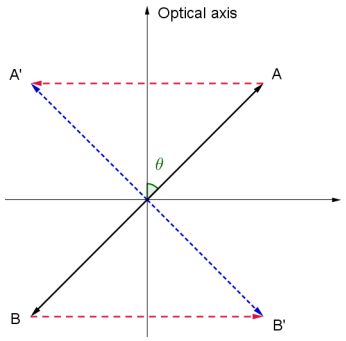

Figure 2.5: When light passes a $\lambda/4$ plate twice, the polarization is rotated 2θ around the optical axis. The black line is the polarization before passing the wave-plate twice. The two points A, B are mirrored to A', B', and the polarization after passing the wave-plate twice is the dotted blue line.

To measure the reflected intensity, it is necessary to split the beam into an in- and outcoming beam. This is done with the polarizing beam splitter (PBS) and $\lambda/4$-plate combination.
The beam-splitter is aligned with the tunable laser's polarization axis. When the light reaches the PBS, it is transmitted, because the polarization matches the beam splitter's transmission axis. The light then goes trough the $\lambda/4$-plate. This introduces a phase shift of $\frac{\pi}{2}$ in one polarisation, and no phase shift in the other. The reflected light crosses the $\lambda/4$-plate again, meaning that one polarization now has a phase shift of π. This polarization changes sign as $e^{i\pi} = -1$. A $\lambda/4$-plate,

just as the PBS, has an optical axis.
It is only the light that couples to this axis that experience the phase shift. This is seen in Figure 2.5
If the $\lambda/4$-plate is placed with an angle of 45° to the PBS, the reflected beam has a polarization perpendicular to the axis which transmits. This means it is reflected, as seen in Figure 2.4.
Before the light reaches the PBS it is Electro-Optically modulated for sideband generation. This technique is described in Section 2.2. The modulation, and demodulation in the mixer produces a DC electric signal, rather than a oscillating signal. This is described in more detail in Section 2.4. The amplitude of the de-modulated signal depends on how far from resonance the carrier frequency is.

When the laser is tuned to resonance, it transmits light. In Figure 2.6 the transmission profile from the optical cavity is seen.

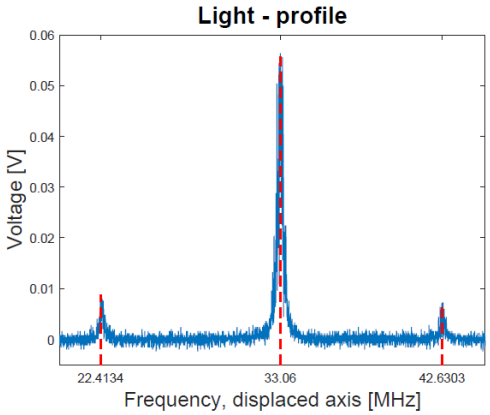

Figure 2.6: This is a frequency scan measured in Diode 1 in Figure 2.4. The frequency axis does not display the actual frequency, but the difference between the central frequency from the laser, and the modulation sidebands. It is seen that the transmitted light has two sidebands with frequency $\omega_\Omega = \omega_0 \pm \Omega$.

The transmitted signal is not suited as an error-signal because the signal has the same sign for a positive and negativ error. The reflection signal in Figure 2.7 is better suited.

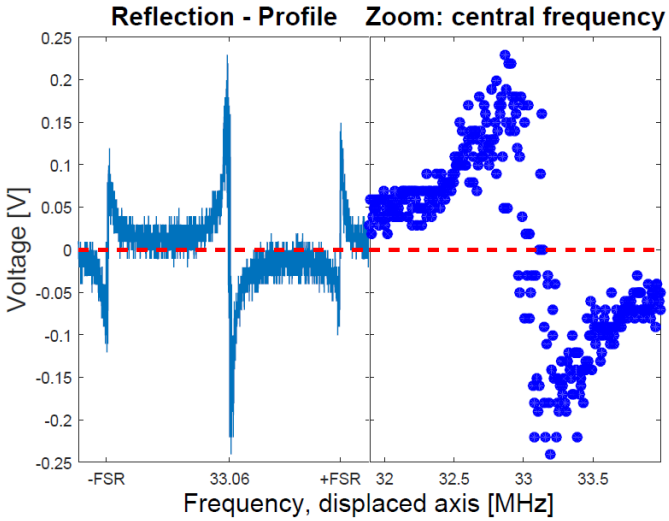

Figure 2.7: This is the mixed signal from Diode 2 and the RF-generator in Figure 2.4. The central frequency and its sidebands are still recognizable. The reflection profile to the left, looks much different than the transmission profile. At resonance the signal is zero, and the sign depends on which way the frequency drifts. To the right is a zoom displayed which makes the slope visible. The voltage corresponding to a drift of 250 kHz is approximately 150 mV. This is why amplification and the PID is needed.

The reflection profile satisfies all three requirements of an error-signal: zero signal at resonance, a steep slope around resonance and sign-dependence of the drift direction.

2.4 Cavity-atom system and detection

Before entering the cavity-atom system the light is sent trough an EOM driven with $\Omega = 500\text{MHz}$. This generates the sideband frequency components, as seen in figure 2.3. It is important to remember that the sidebands are 180° out of phase with each other.

As the light in the experiment is supposed to drive the ${}^1S_0 \rightarrow {}^3P_1$ transition of strontium which is visible red light with $\lambda = 689.3$ nm, the frequency is on the order of $\nu = \frac{c}{\lambda} \approx \frac{10^8}{10^{-7}} s^{-1} \approx 400\text{THz}$. The diodes cannot measure a signal this fast. Instead of measuring the signal at the three specific frequencies, it is the beat signal between the carrier frequency and the sidebands which is measured. When viewed as a real signal composed of sines, the beat signal is given by

$$\begin{aligned} E &= E_0 \cdot J_0(\beta)\sin(\omega_0 t) + E_0 \cdot J_1(\beta)\sin((\omega_0 + \Omega)t) \\ &= A \cdot (\sin((\omega_0 + \omega_0 + \Omega)t)\sin((\omega_0 - \omega_0 - \Omega)t) \\ &\approx A \cdot \sin(\Omega t) \end{aligned} \tag{2.5}$$

where A is the amplitude of the beat signal. The first frequency part varies too fast for the sensor to measure and is not seen. The same result is obtained for the second beat signal, only with a difference in sign, which can be seen from equation (2.4). If measured directly after the EOM in Figure 2.2, the signal at 500 MHz would be zero, as the two beats cancel each other out.

When the light enters the cavity containing the strontium atoms, it is only the carrier frequency component which interacts with the atoms, as it is almost on atomic resonance with the ${}^1S_0 \rightarrow {}^3P_1$ transition. The two sidebands are off resonance with the atoms, and stay 180° out of phase with each other.
As seen in Figure 2.2 the light enters the strontium filled cavity, and the outcoming intensity is measured. To calculate this intensity, the electric field of each frequency component is calculated individually.
The cavity, as seen in Figure 2.8, consists of two equal mirrors. Equal means their reflection and transmisson coefficients r,t are the same. When the light is transmitted into the cavity it decreases by a factor of t. The same happens when transmitted out. The light which is not transmitted takes one round trip in the cavity, and hereby decreases by a factor r^2. This cycle is infinite.
The phase also changes. There is two contributions; the distance L travelled and a phase shift $\beta_0$due to the atoms. For every round trip m the distance is $s = 2L$. Formally this can be written as

$$\begin{aligned} E_{out} &= E_{in} \cdot t^2 \cdot (e^{ikL+\beta_0} + r^2 e^{i(3kL+3\beta_0)} + r^4 e^{i(5kL+5\beta_0)} + ...) \\ &= E_{in} t^2 e^{i(kL+\beta_0} \cdot (1 + \sum_{m=1}^{\infty} r^{2m} e^{2mi(kL+\beta_0)}) \\ &= E_{in} \frac{t^2 e^{i(kL+\beta_0)}}{1 - r^2 e^{i2(kL+\beta_0)}} \end{aligned} \tag{2.6}$$

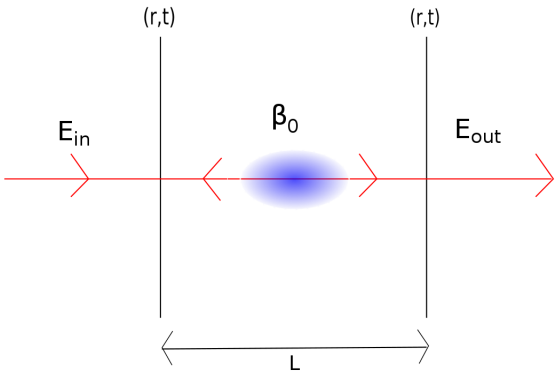

Figure 2.8: A Cavity with atoms. The two mirrors are identical, i.e. r,t are the same for the two mirrors. The phase of the light depends on the number of trips in the cavity the photons take. This is statistically determined by r and t. The phase β_0 also depends on the coupling with the atoms.

The resonance of the cavity-atom system is given by the resonance condition

$$\begin{aligned} 2k_{res}L + 2\beta_0 &= m2\pi \\ \omega_{res} &= \frac{m\pi c}{L} - \frac{\beta_0 c}{L} \end{aligned} \tag{2.7}$$

β_0 is the phase shift of the carrier frequency due to the atoms. The experiment is designed to lock the carrier frequency on resonance with the cavity-atom system. The mechanism is the feedback

loop to the AOM in Figure 2.2. It is seen that there are two components of the resonance; the free spectral range of the cavity $FSR = \frac{m\pi c}{L}$ and a detuning caused by the atoms $\delta = -\frac{\beta_0 c}{L}$. From this relation it is possible to determine the frequency of the sidebands, since they are one FSR displaced from the cavity-atom resonance.

$$\omega_\Omega = \frac{(m \pm 1)\pi c}{L} - \frac{\beta_0 c}{L} \tag{2.8}$$

From equation (2.6) the electric field out of the cavity is determined for the sideband frequencies. Since the sidebands are far of atomic resonance with the strontium atoms, they experience no phaseshift which means $\beta = 0$. The wave-vector for the sidebands is found from equation 2.8

$$E_{out} = E_{in}\frac{t^2 e^{ik_\Omega L}}{1 - r^2 e^{i2k_\Omega L}} \tag{2.9}$$

$$= E_{in}\frac{t^2 e^{i(\frac{(m\pm1)\pi c}{L} - \frac{\beta_0 c}{L})\frac{L}{c}}}{1 - r^2 e^{i2(\frac{(m\pm1)\pi c}{L} - \frac{\beta_0 c}{L})\frac{L}{c}}} \tag{2.10}$$

$$= E_{in}e^{i(m\pm1)\pi} \cdot \frac{t^2 e^{-i\beta_0}}{1 - r^2 e^{i2(m\pm1)\pi} e^{-2i\beta_0}} \tag{2.11}$$

In equation (2.11) the phase factor in front is -1 for m even, and 1 for m uneven. For all m the first complex phase in the denominator will be e to an even number of 2π, which is 1. The outcoming E-field is described by the complex number z

$$E_{out} = \pm E_{in} \cdot \frac{t^2 e^{-i\beta_0}}{1 - r^2 e^{-2i\beta_0}} = E_{in} z = E_{in}|z|e^{i\phi_\Omega} \tag{2.12}$$

The sidebands experience a phase shift of $\phi_\Omega = Arg(\frac{t^2 e^{-i\beta_0}}{1-r^2 e^{-2i\beta_0}})$. Note, that the transmitted carrier-signal does not experience any phase shift because it is locked on resonance with the total cavity-atom system. ϕ_Ω is the phase difference between the transmitted sideband and carrier frequencies.
When disregarding all loss trough the cavity, the total transmitted electric field is, from equation (2.4)

$$E_{out,total} = E_0 \cdot (J_0(\beta)e^{i\omega_0 t} + J_1(\beta)(e^{i((\omega_0+\Omega)t+\phi_\Omega)} - e^{i((\omega_0-\Omega)t+\phi_\Omega)})) \tag{2.13}$$

When the signal is measured it is the intensity that is measured. The complete derivation for this signal can be reviewed in Appendix A

$$I_{out,total} \sim E_{out,total} \cdot E^*_{out,total}$$
$$= C - 2J_1^2 \cos(2\Omega t) + 4J_0 J_1 \sin(\Omega t)\sin(\phi_\Omega) \tag{2.14}$$

The constant C only contains information on the laser intensity which we are not interested in. The fast oscillating signal's frequency is higher than the sensors bandwidth, and is not measured. Then equation (2.14) becomes

$$I_{out} = 4J_0 J_1 \sin(\Omega t)\sin(\phi_\Omega) \tag{2.15}$$

As seen in Figure 2.2 this signal is mixed with the output from the Ω sideband frequency control RF-signal. The mixed signal is

$$\begin{aligned} S_{mixed} &= (-2J_1^2\cos(2\Omega t) + 4J_0J_1\sin(\Omega t)\sin(\phi_\Omega))e^{i\Omega t} \\ &\propto k_1 e^{i3\Omega t} + k_2 e^{i2\Omega t} + k_3 e^{i\Omega t} + k_4\sin(\phi_\Omega) \end{aligned} \tag{2.16}$$

With a low-pass filter the DC-signal is isolated and used as the error signal

$$S_{low-pass} \propto \sin(\phi_\Omega) \tag{2.17}$$

For a small phase shift, the approximation $\sin(\phi_\Omega) \approx \phi_\Omega$ is made, and the error-profile has the same shape as the dispersion profile.

2.5 Phase measurement profile

The phase difference ϕ_Ω is a result of atom-light interactions between the carrier frequency and the strontium atoms in the cavity, and the non-existing interaction for the sidebands. This arises as a consequence of dispersion. The frequencies see a different refraction index n, which means their optical path length is different according to $OPL = nl$. This phase difference is proportional to

$$\phi_\Omega \sim n_0 l - n_\Omega l = l(n_0 - n_\Omega)$$

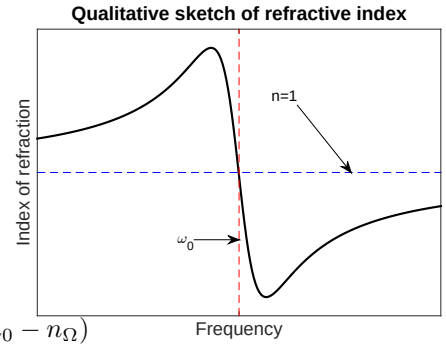

Figure 2.9: Example of dispersion profile

Since the cavity is sitting in a vacuum, and the sidebands are far from the very narrow resonance of the ${}^1S_0 \rightarrow {}^3P_1$ transition, the refractive index n_Ω is 1. When applying the model for the refractive index for a gas [9], the phase difference is

$$\phi_\Omega \sim \frac{lNq^2}{m_e\epsilon_0}\frac{(\omega_{res}^2 - \omega_0^2)}{(\omega_{res}^2 - \omega_0^2)^2 + \gamma^2\omega_0^2} \tag{2.18}$$

The dispersion profile is qualitatively shown in Figure 2.9.
In equation (2.18) l is the length of the strontium gas cloud in the propagatio axis, N is the atomic density in the cavity, q is the elementary charge, m_e is the electron mass, ϵ_0 the vacuum permitivity, ω_0 is the carrier frequency, and ω_{res} is the resonance for the cavity-atom system. γ_k is a damping constant which corresponds to absorption and spontaneous emission in the atom cloud. This effect has been neglected so far, but has a large effect on the refractive index. If absorption is not considered, the refractive index would become asymptotically unstable around resonance. Because the strontium gas is not cooled to excactly 0 K, the atoms move around.

This introduces a number of doppler effects. A regular doppler-shifted broadening, and a number af mechanisms in which the atoms can absorb photons, which are velocity dependent. The effect of this is seen in Figure 2.10

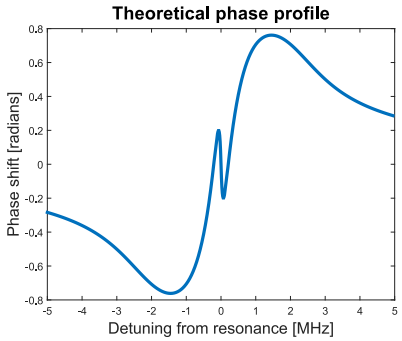

Figure 2.10: The phase profile changes when considering doppler-effects. The slope around the atom-cavity resonance is now even steeper, which means the error-signal has improved. This is a numerically calculated theory, with data from [10].

3 Residual amplitude modulation

One of the main sources of noise in the experiment is Residual Amplitude Modulation, in short RAM. This effect comes from the Electro-Optic Modulation described in 2.2. There are two origins of the RAM; the performance of the EOM-device[11] and disturbances from the environment.
The detection method as described in Section 2.4, is to measure the phase of the beat signal between the sidebands and the carrier after the interaction with the Sr-atoms. This builds on the assumption that the two sidebands are 180°out of phase before the atom-interaction, which is also the ideal result from electro-optic modulation. In the lab, this is not the case.
If the laser is tuned to resonance, the sidebands are not phaseshifted. Ideally they have a phase difference of $\phi = \pi$. But the RAM introduces a phase difference θ before the cavity, which means $\phi \neq \pi$. The feedback interprets this as if the carrier is off resonance and stabilizes to $\phi = \pi + \theta$ instead of $\phi = \pi$. θ is not constant, it drifts in time. This leads to a drift in the carrier frequency, as seen in Figure 3.1, which means the laser has different frequencies at different times, i.e. not a stable laser.

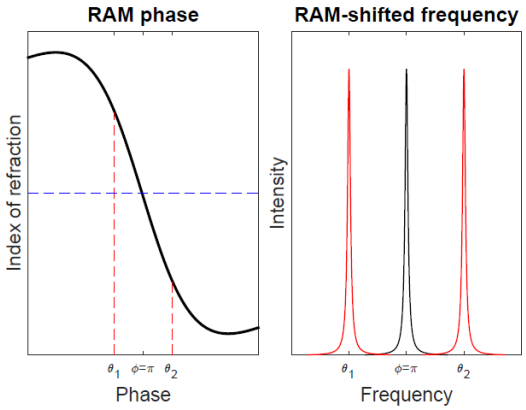

Figure 3.1: To the left is shown an example of a stabilized laser, where the phase difference between the sidebands is shifted $\theta_{1,2}$. To the right, the RAM shifted frequencies are shown.

The RAM signal arises from the EOM's performance. Inside the EOM, the light couples to a crystal. When the crystal is exposed to an electric potential, the electrons respond, and the crystal grid changes. This changes the refractive index and the light gains a phase when traveling trough the crystal. The electric potential can be varied as seen in Figure 3.2. In this experiment a signal from an RF-generator is used to modulate the electric potential. The refractive index is a linear function of the electric potential $n = kV(t)$. This is the physical foundation of equation (2.1), where $V = k\sin(\Omega t)$.

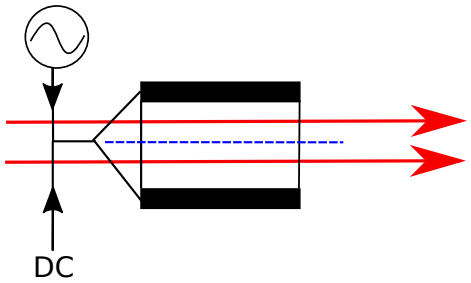

Figure 3.2: This is a cross section of the EOM. The red light travels in the crystal. The two outer black boxes are metal plates. The electric potential across the crystal is symmetric around the dotted line, which is the center of the crystal. It is not completely uniform though, which means the phaseshift depends on lights path trough the crystal. This effect is disregarded.

Because the crystal has two different refractive indices, it acts as a waveplate. Not like a $\lambda/4$ plate as used in the expriment, but the polarization is changed trough an angle θ_{RAM}. A waveplate's effect is frequency-dependent. Because the three components have different frequencies, their polarization varies individually. Only when the beat-signals are aligned they cancel out, as seen in Figure 3.3.

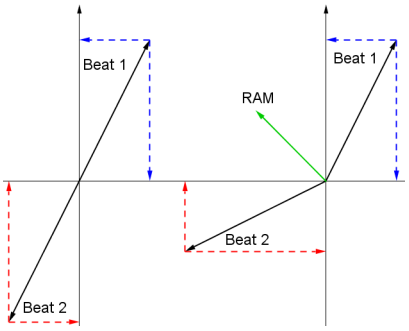

Figure 3.3: To the left, the two beat signals are in phase and aligned. They cancel out completely. To the right the beat signals are in phase but not aligned. They do not cancel out.

3.1 RAM control

The misalignment of the two beat signals after the EOM leads to RAM given by [12]

$$\begin{aligned} RAM &= -\sin(2\beta)\sin(2\gamma)|\epsilon_0|^2 J_1 \sin(\Omega t)\sin(\theta_{RAM}+\phi_0) \\ &= c_{pol} A \sin(\Omega t)\sin(\theta_{RAM}+\phi_0) \end{aligned} \tag{3.1}$$

where c_{pol} is a polarisation factor from the in- and outcoming surface, A the amplitude, ϕ_0 is a phase shift induced by adding a DC-component to the modulating signal sent into the EOM. θ_{RAM} is the unwanted phase shift caused by the natural birefringence of the crystal, which is temperature T dependent [13].

$$\theta_{RAM}(T) = \frac{2\pi l}{\lambda}(n_e(T) - n_0(T)) \tag{3.2}$$

If $\sin(\theta_{RAM}+\phi_0) = 0$, the RAM signal would be zero

The refractive indices are approximately linearly temperature-dependent.
The approach to eliminate the RAM signal has two steps. First step is a temperature stabilization of the EOM. The second step is to add a DC-control signal to supply the needed ϕ_0. When temperature stabilization is on, the temperature drift is only ± 2.2 mK when measured over 15 hours. The DC-control setup is shown in Figure 3.4

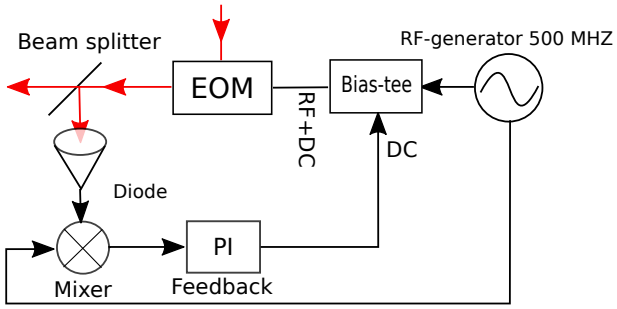

Figure 3.4: The bias-tee sums the RF and the DC signal. The diode measures the beat signal. If it is non-zero, it is sent trough a Proportional Integrator circuit and into the EOM to stabilize the output.

An example of a RAM measurement is given in Figure 3.5. It varies slowly and sinusoidally at a frequency of approximately 0.5 Hz.

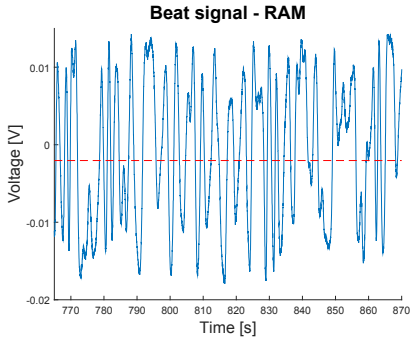

Figure 3.5: The RAM signal is varying sinusoidally at approximately 0.5 Hz. The measurement is taken after the modulation in the mixer.

3.2 RAM error signal and feedback control

The RAM error signal is seen in Figure 3.5. This voltage-signal is sent to a proportional-integrator circuit. There are 4 parts in this PI-controller: An inverting amplifier, a proportional integrator, a voltage follower and a current booster. The amplifications are needed to make the control signal large enough for the EOM to compensate. The integrator accelerates the stabilization as an error with the same sign over time is integrated to a higher voltage.
The resistance of the plates inside the EOM is very small. Ohm's law dictates that the EOM is supplied with a large current to give the needed high compensating DC-voltage. The complete control circuit is designed only to respond to slow frequency-signals from the surroundings, and not the high-frequency electronic noise from sensors etc. The circuit is sketched in Figure 3.6

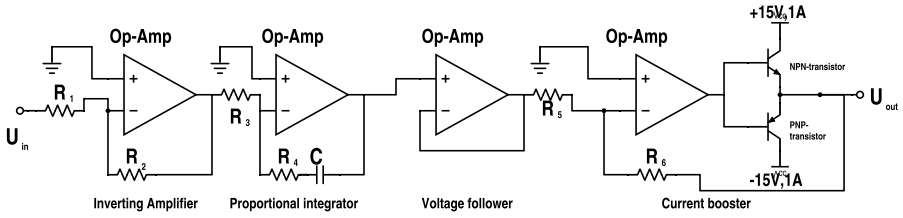

Figure 3.6: The inverting amplifier multiplies the signal with the gain factor G that is given as the ratio of the resistors $G = -\frac{R_2}{R_1}$. The PI also contributes a gain factor, while also integrating the signal $U_{PI} = -\frac{R_4}{R_3}\int_0^t U$. The voltage follower does nothing to the signal, but it is ready to supply current if the output is loaded heavily. The current booster does not change the voltage because $R_5 = R_6$.

3.3 Allan Variance

To estimate the stability of a system, the Allan variance is often used as a good measure. Instead of calculating the standard deviation which contains information about the global data set, the Allan variance compares a measurement to its adjacent measurements. A slow linear drift will give a large Allan variance for longer time scales, because the first measurements will be below the global

mean, and the last will be above. The Allan variance for short timescales will be smaller, as the drift is smaller than the noise of a system. In this sense the Allan variance contains information on the sort of noise in a data set. It is also known as the two sample variance, because it only compares two adjacent samples. Mathematically this is described as [14]

$$\sigma^2_{Allan}(\tau) = \frac{1}{2}\left\langle (\overline{y_2(\tau)} - \overline{y_1(\tau)})^2 \right\rangle \tag{3.3}$$

The Allan deviation is just the square root of the variance

$$\sigma_A(\tau) = \sqrt{\sigma^2_{Allan}(\tau)} \tag{3.4}$$

The brackets in equation (3.3) mean that it is the mean of the difference of all adjacent measurement pairs. The Allan variance can also be calculated for longer time scales. Instead of using all the individual measurements, they are binned as the mean of τ adjacent measurements. This corresponds to a longer sampling time. If a drift is small, it is not significant compared to noise on short timescales. For larger τ, a drift is dominant because noise is equally distributed above and below the mean.
When raising τ, the averaged measurements are removed from each other in time. For a given τ the drift becomes larger than the noise, which means the Allan deviation increases. It is this turning point which describes a system's long-term stability.
In Figure 3.7 and 3.8 the Allan deviation for computer-generated data series is shown. From equation (3.2) we expect a linear phase drift. From equation (3.1) this leads to an oscillating RAM-signal. The MatLab script used to calculate the Allan deviation is shown in Appendix B

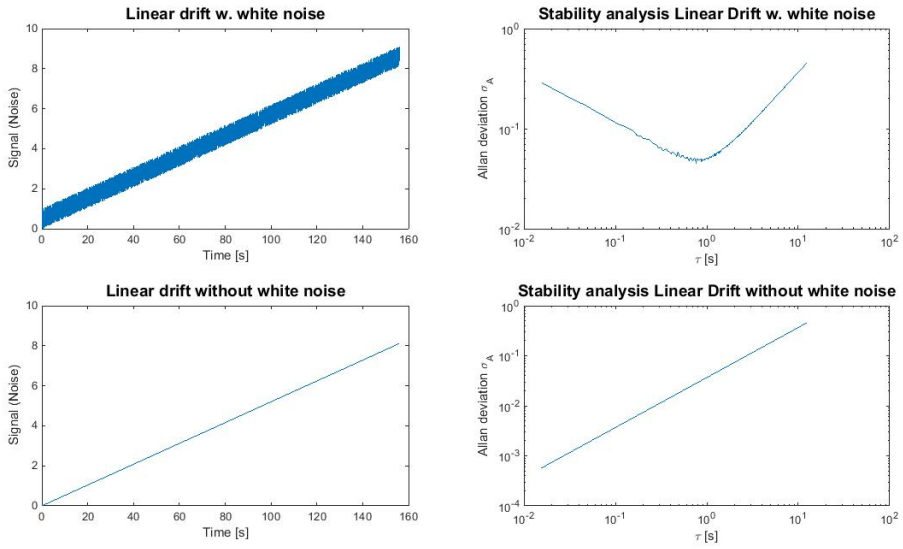

Figure 3.7: A computer model for a linear drift. The top graphs show a signal with white noise. The stability point is recognized as the point where the Allan deviation breaks off. The presence of white noise is seen in the negative slope for low τ

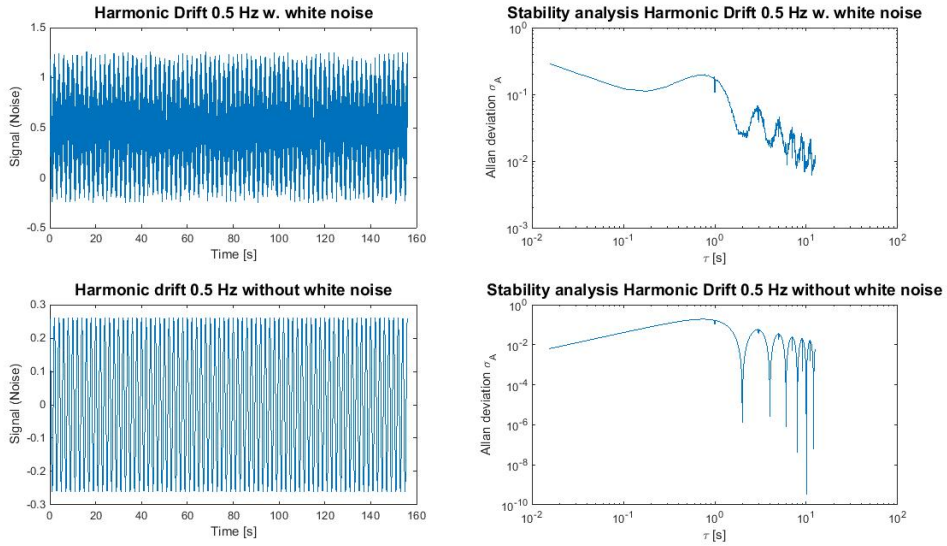

Figure 3.8: The expected RAM-signal profile. If it is only a linear drift in the EOM-crystal temperaure which causes the RAM, a harmonic oscillation profile would be the result. The white noise regime for low τ is easily recognizable, in the top right graph.

4 Data analysis and discussion

The key to a stable laser is an error-signal with a good signal to noise ratio. The error-free signal is achieved by having very stable noise suppresion mechanisms. The performance of the PDH-lock and the RAM-suppresion is essential to a stable carrier frequency stabilization. In this section, the stability of the PDH-lock and the RAM-feeback is examined.

4.1 PDH-lock stability

The method of determining the performance of a feedback system is to measure the stability of the error-signal. When the error-signal is non-zero, stability decreases. A good feedback mechanism corrects the drift before the error-signal drifts far away from zero.

A measurement of the error-signal in the PDH lock is shown in Figure 4.1. The error-signal is a voltage which corresponds to a frequency-drift. To translate between the two, the error-signal profile (Figure 2.7) is used. The oscillations are on the order of 100 kHz.

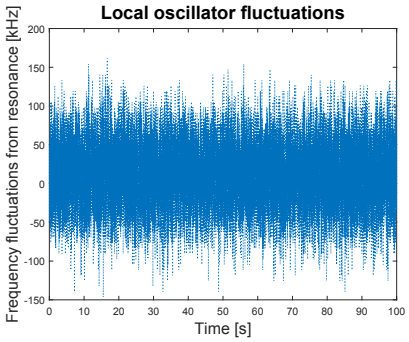

Figure 4.1: Measurement of the PDH-lock error signal. The laser drifts ±100 kHz in frequency. This plot only shows how much the frequency drifts, but not which kind of noise it is.

To determine if the PDH-lock is working, the Allan-deviation is plotted in Figure 4.2. The Allan deviation profile matches a white-noise signal. This means the PDH-lock suppresses regular drifts. On long time scales, i.e 10 s, the signal starts to oscillate, but the amplitude of the oscillation is very small. It is the white noise that is the main noise component, and not a systematic drift.

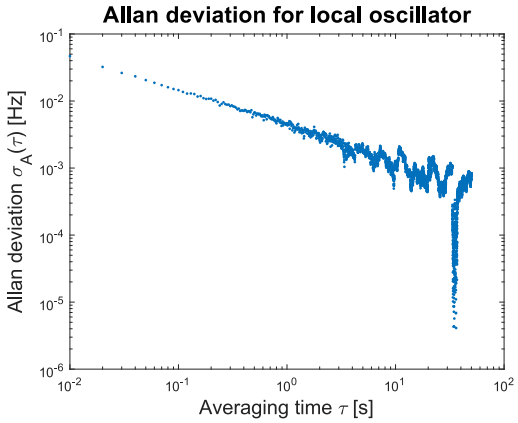

Figure 4.2: The Allan deviation profile matches a white noise signal. There is also a slow oscillating drift of approxiamtely 0.1 Hz, but it is very small in amplitude, and the white noise signal dominates. The PDH-lock suppresses drifts caused by the surroundings, and effects inside the tunable laser.

4.2 RAM stability

The main focus of this project was to stabilize the RAM. With temperature stabilization, but without feedback to the EOM, the RAM signal was shown in Figure 3.5. The phase shift induced by the feedback is voltage-dependent. Because the EOM draws a lot of current, the fear of an overcurrent limits the maximum phase shift $\phi_{0,max} \sim R_{EOM} \cdot I_{limit}$. To compensate for all RAM phaseshifts a voltage corresponding a phase ϕ, $V_\pi = 6$ V [15], is needed. The upper voltage limit is kept lower than 6 V, which means the stabilization only works in a dynamical regime. This causes the RAM-lock to switch on and off, as seen in Figure 4.3.

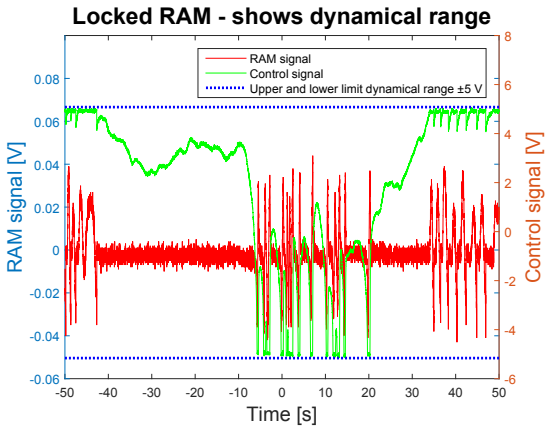

Figure 4.3: This plot shows the locked RAM signal and the corresponding control signal. When the control signal is non-zero, it compensates RAM. At the limits of the control signal the lock falls of, and the RAM begins to oscillate.

In most stabilizations, the servo-mechanism locks a physical variable, such as temperature. In this RAM control, the temperature control already locks the EOM's physical environment. The DC-control signal can only compensate the error, not lock it to zero. Because there is an upper and lower limit to this compensation, the RAM lock is not perfect.

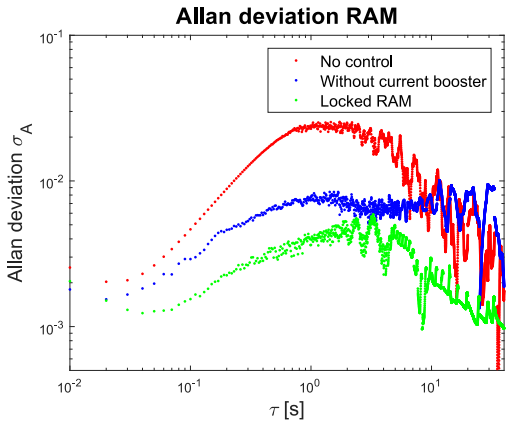

Figure 4.4: The red curve is the Allan deviation of the RAM signal. On very short timescales it is dominated by white noise. As expected it has an oscillating profile on longer timescales. When RAM control is applied (blue curve) the profile is lowered. On longer timescales it does not oscillate but rather stays constant. The Allan deviation for the current boosted control is the green curve. The stability has increased by one order of magnitude.

The first control-circuit produced was without a current booster, which meant the dynamical range of RAM control was smaller. In Figure 4.4 the Allan deviation for the non-applied, non-boosted and boosted RAM-control is seen.
The stability of the RAM signal on long timescales increases in the periods where the lock is on. To get an estimate of the Allan deviation if the dynamical range was $[-V_\pi, V_\pi]$, the Allan deviation is calculated for a RAM-locked interval, from [-40,-10]s in Figure 4.3. If the RAM is completely

locked, the dominant noise source in the measurement should be flicker noise from the electronic equipment.

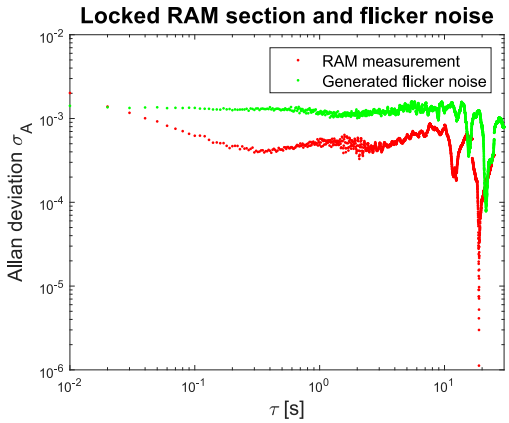

Figure 4.5: The red curve is the Allan deviation for a RAM locked section inside the control signal's dynamical range. The green curve is the Allan deviation for a computer generated flicker noise series [16] without white noise. On short timescales the RAM signal is dominated by white noise. Then there is a regime dominated by the oscillating drift. On long timescales it has the sudden drops corresponding to flicker noise.

If it is possible to expand the dynamical range to $[-V_\pi, V_\pi]$, a lower noise limit dominated by the photodiode's and electronic devices' flicker noise can be approached. The Allan deviation for this locked section is two orders of magnitude lower than for the un-controlled RAM on long time scales.

The RAM-control developed in this project is well suited to supress noise in the EOM. In the experiment the light is guided around the lab in polarizing-maintaining optical fibers. Inside a PM-fiber the light travels trough a wave-guide with birefringence, just as the EOM-crystal. When the fibers are subjected to stress or quick temperature changes the RAM-control fails. Figure 4.6 shows the RAM with active control. The oscillations starts when the fiber is touched by a finger.

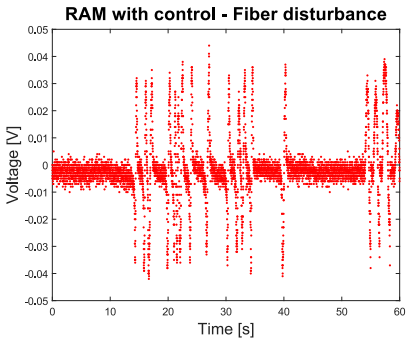

Figure 4.6: The RAM control fails when the optical fiber are exposed to external stress and quick temperature changes. The disturbance happens at t= 15 s and t= 55 s.

5 Conclusion

In this project, a Residual Amplitude Modulation control method has been developed. The RAM introduces noise in a phase measurement used to stabilize a laser. The RAM is lowered by one order of magnitude, which improves the signal-to-noise relationship of the final laser stabilization signal. The RAM control's performance is limited by the dynamical regime of the control signal. Measurements for a time-period of 30 seconds where the RAM-control is in the dynamical regime, indicates that the lower limit for the noise is two orders of magnitude lower than without control.

6 References

[1] Bondarescu, R., "Geophysical applicability of atomic clocks: direct continental geoid mapping"
Geophysical Journal International, **191**, 78-82, October 2012

[2] Graham, P. W., "New method of gravitational wave detection with atomic sensors"
Physical Review Letters, **110**, 171102, April 2013

[3] Prestage, J. D., "Atomic clocks and variations of the fine structure constant"
Physical Review Letters, **74** (18), May 1995

[4] Black, E. D., "An introduction to Pound-Drever-Hall laser frequency stabilization"
American Journal of Physics **69**, (79) (2001)

[5] Milonni, P. W., "Laser Physics" *Wiley*, 2010

[6] Ye, J., Ma, L., Hall, J. L., "Ultrasensitive detections in atomic and molecular physics: demonstration in molecular overtone spectroscopy"
Journal of the Optical Society of America B **Vol. 15, No. 1,** January 1998

[7] Riley, K. F., Hobson, M. P., "Essential mathematical methods for the physical sciences"
Cambridge University Press, 2011

[8] Foot, C. J., "Atomic Physics" *Oxfor University Press*, 2005

[9] Griffiths, D. J., "Introduction to Electrodynamics 4th edition" (Section 9.4)
Pearson, 2013

[10] Westergaard, P. G., et al., "Obervation of motion-dependent nonlinear dispersion with narrow-linewidth atoms in an optical cavity"
Physical Review Letters, **114**, 093002, March 2015

[11] Whittaker, E. A. et al., "Residual amplitude modulation in laser electro-optic phase modulation"
Journal of the Optical Society of America B **Vol. 2, No. 8,** August 1985

[12] Zhang, W. et al., "Reduction of residual amplitude modulation to $1 \cdot 10^{-}6$ for frequency modulation and laser stabilization"
Optics Letters **39,** April 1, 2014

[13] Li, Liufeng. et al., "Measurement and control of residual amplitude modulation in optical phase modulation"
Review of Scientific Instruments **83,** 043111, April 19, 2012

[14] Riehle, F.., "Frequency Standards"
Wiley 2004

[15] Jenoptik, "Integrated-optical modulators - Technical information"
`http://www.jenoptik.com/cms/products.nsf/0/F1ADB2DABE5528A9C1257CE0002C4CA9/$File/modulatorfibel_en.pdf?Open`

[16] Baranski, P., "Pink (flicker) noise generation"
Matlab Central File Exchange, `http://www.mathworks.com/matlabcentral/fileexchange/34467-pink--flicker--noise-generator`, 2012. Downloaded April 14 2015

A Intensity signal from strontium filled cavity calculation

This is the total derivation of the transmission signal

$$\begin{aligned}
I_{out,total} &= E_{out,total} \cdot E^*_{out,total} \\
&= E_0^2 \cdot e^{i(\omega_0-\omega_0)t} \cdot (J_0 + J_1(e^{i(\Omega t+\phi_\Omega)} - e^{i(-\Omega t+\phi_\Omega)})) \\
&\quad \cdot (J_0 + J_1(e^{-i(\Omega t+\phi_\Omega)} - e^{-i(-\Omega t+\phi_\Omega)})) \\
&= E_0^2(J_0^2 + 2J_1^2 - 2J_1^2(e^{i2\Omega t} + e^{-i2\Omega t}) + J_0J_1(e^{i(\Omega t+\phi_\Omega)} + e^{-i(\Omega t+\phi_\Omega)} \\
&\quad - e^{i(-\Omega t+\phi_\Omega)} - e^{-i(-\Omega t+\phi_\Omega)})) \\
&= C - 2\cos(2\Omega t) + 2J_0J_1(\cos(\Omega t+\phi_\Omega) - \cos(-\Omega t+\phi_\Omega))
\end{aligned}$$

The constant only contains information about the laser intensity which we are not interested in, and the fast oscillating signal's frequency is higher than the sensors bandwidth. Then equation (2.14) becomes

$$\begin{aligned}
I_{out} &= J_0J_1(e^{i\Omega t}e^{i\phi_\Omega} + e^{-i\Omega t}e^{-i\phi_\Omega} - e^{-i\Omega t}e^{i\phi_\Omega} - e^{i\Omega t}e^{-i\phi_\Omega}) \\
&= J_0J_1(e^{i\phi_\Omega}(e^{i\Omega t} - e^{-i\Omega t}) - e^{-i\phi_\Omega}(e^{i\Omega t} - e^{-i\Omega t})) \\
&= 2J_0J_1\sin(\Omega t)(e^{i\phi_\Omega} - e^{-i\phi_\Omega}) = 4J_0J_1\sin(\Omega t)\sin(\phi_\Omega)
\end{aligned}$$

B Allan deviation MatLab script

The Matlab script used to calculate the Allan deviation is

```
function [allan_deviation,allan_variance,tau] = allan(data,time_diff,tau_max)

% time_diff is the sampling time
% tau_max is the maximum number of measurements in a binning

data_var = zeros(tau_max,1);

for j = 1:tau_max
    data_allan = zeros(floor(length(data)/j-1),1);

    for i = 1:length(data)/j-1
        data_allan(i) = (mean(data(j*i+1:j*i+j)) - mean(data(j*i-j+1:j*i)))^2;
    end

    data_var(j) = 1/2*mean(data_allan);

    data_allan = [];
end

allan_variance = data_var;
allan_deviation = sqrt(allan_variance);

tau = zeros(tau_max,1);
for i = 1:tau_max
    tau(i) = i*time_diff; % the new time axis
end
```